

*Advanced* 

# Synthesis & Catalysis

## Accepted Article

**Title:** Stable Zero-Valent Nickel Nanoparticles in Glycerol: Synthesis and Applications in Selective Hydrogenations

**Authors:** Antonio Reina, Isabelle Favier, Christian Pradel, and Montserrat Gómez

This manuscript has been accepted after peer review and appears as an Accepted Article online prior to editing, proofing, and formal publication of the final Version of Record (VoR). This work is currently citable by using the Digital Object Identifier (DOI) given below. The VoR will be published online in Early View as soon as possible and may be different to this Accepted Article as a result of editing. Readers should obtain the VoR from the journal website shown below when it is published to ensure accuracy of information. The authors are responsible for the content of this Accepted Article.

**To be cited as:** *Adv. Synth. Catal.* 10.1002/adsc.201800786

**Link to VoR:** <http://dx.doi.org/10.1002/adsc.201800786>

DOI: 10.1002/adsc.201((will be filled in by the editorial staff))

# Stable Zero-Valent Nickel Nanoparticles in Glycerol: Synthesis and Applications in Selective Hydrogenations

Antonio Reina,<sup>a</sup> Isabelle Favier,<sup>a</sup> Christian Pradel,<sup>a</sup> and Montserrat Gómez<sup>a\*</sup>

<sup>a</sup> Laboratoire Hétérochimie Fondamentale et Appliquée, Université de Toulouse 3 - Paul Sabatier, UPS and CNRS UMR 5069, 118 Route de Narbonne, F-31062 Toulouse Cedex 9, France  
[Phone : +33 561557738, Fax : + 33 561558204, e-mail : gomez@chimie.ups-tlse.fr]

Received: ((will be filled in by the editorial staff))

Supporting information for this article is available on the WWW under <http://dx.doi.org/10.1002/adsc.201#####>. ((Please delete if not appropriate))

**Abstract.** Small (mean diameter, *ca.* 1.2 nm) and well-dispersed zero-valent nickel nanoparticles (NiNPs) stabilized by cinchona-based alkaloids and TPPTS (tris(3-sulfophenyl)phosphine trisodium salt), were synthesized from the organometallic precursor [Ni(cod)<sub>2</sub>] in neat glycerol under hydrogen pressure. NiNPs were fully characterized ((HR)-TEM, EDX, XPS, XRD, IR, magnetization), both at solid state and directly from the corresponding colloidal solutions in glycerol due to its negligible vapour pressure. NiNPs dispersed in glycerol were applied in hydrogenation reactions, in particular in semihydrogenation of alkynes to give (*Z*)-alkenes under satisfactory conditions (3 bar H<sub>2</sub>,

1 mol% Ni, 100 °C), showing remarkable activity and selectivity. The catalytic phase was recycled at least ten times without loss of activity, affording in each case metal-free organic products. Other functional groups such as nitro, nitrile and formyl groups were efficiently hydrogenated to the corresponding anilines, benzylamines and benzylalcohols (77-95% yields).

**Keywords:** Nickel; Nanoparticles; Glycerol; Hydrogenation; Semihydrogenation of alkynes; Catalyst recycling

## Introduction

The selective hydrogenation of carbon-carbon triple bonds is a very valuable tool in organic synthesis because alkenes are useful building blocks, both at laboratory and industrial scale.<sup>[1]</sup> In particular, this process represents a crucial step in polymerization reactions in order to eliminate alkynes and dienes from alkene raw materials.<sup>[2]</sup> The two main challenges rely on controlling the stereochemistry and avoiding over reduction towards the corresponding alkane. For the synthesis of (*Z*)-alkenes from internal alkynes and also for the synthesis of alkenes from terminal alkynes, several methodologies have been applied, such as i) Lindlar catalyst,<sup>[3]</sup> including lead-free metal-based systems;<sup>[4]</sup> ii) complex reducing agents of the type NaH-NaOR-MX<sub>n</sub><sup>[5]</sup> and iii) dispersed nickel metal on graphite.<sup>[6]</sup> However, over reduction and isomerization reactions happen and consequently the chemoselectivity is difficult to be controlled. In recent years, nickel catalysts and in particular supported nickel nanoparticles including nickel-based alloys, have been studied, due to their ability to selectively hydrogenate alkynes into alkenes.<sup>[7-13]</sup>

In the last decade, the skillful synthesis of well-defined NiNPs has attracted the attention of several research groups, being the main challenge the exclusive formation of Ni(0) nano-materials due to the easy oxidation of zero-valent nickel species. Some of these methodologies describe the synthesis of Ni-based alloys<sup>[9,11,13,14]</sup> and also nickel nanoparticles supported on different kinds of solids,<sup>[8,12,15-18]</sup> even under continuous millifluidic conditions.<sup>[19]</sup> The lack of control in the oxidation state of the metal in the preformed nano-catalysts is a recurrent reported issue, highlighted by different authors: Tilley *et al.* in the synthesis of nickel nanocubes by reduction of Ni(acac)<sub>2</sub> under hydrogen;<sup>[20]</sup> Hyeon's group in the synthesis of NiNPs prepared under thermal decomposition;<sup>[21]</sup> and Zarbin *et al.* in the synthesis of NiNPs by the polyol methodology.<sup>[22]</sup>

Chaudret's group reported an efficient method for the synthesis of nickel(0) nanorods exhibiting magnetic properties, obtained from [Ni(cod)<sub>2</sub>] under hydrogen atmosphere.<sup>[23]</sup> Based on this procedure, Philippot and co-workers have recently described the preparation of Ni(0)NPs supported on SiO<sub>2</sub> for the catalytic hydrogenation of alkenes.<sup>[24]</sup>

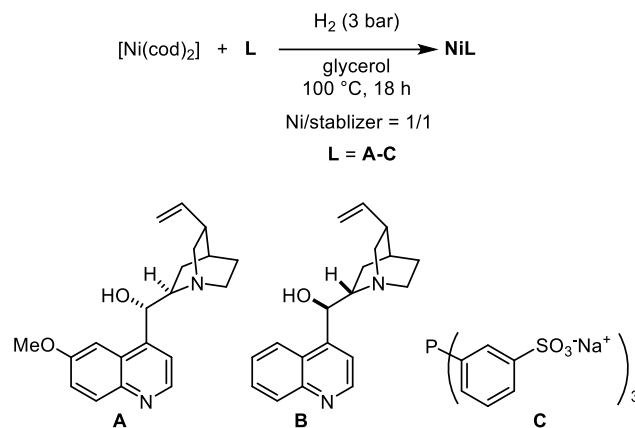
In contrast to the use of NiNPs as solid catalysts, few works have been published in liquid catalytic phase, the main part of them using ionic liquids. Dupont *et al.* synthesized Ni(0)NPs in imidazolium-based ionic liquids which showed a thin layer of nickel oxide, being active in the reduction of alkenes.<sup>[25]</sup> Janiak's group reported the synthesis of small crystalline Ni(0)NPs exhibiting a hcp structure, in imidazolium-, pyridinium- and thiophenium-based ionic liquids under micro-wave conditions.<sup>[26]</sup> Shen's group described the formation of Ni and Ni/NiO core-shell nanoparticles in water using glycerol as co-solvent.<sup>[27]</sup>

In this context, we were interested in the efficient synthesis of zero-valent nickel nanoparticles in neat glycerol based on the methodology previously developed in our group.<sup>[28,29]</sup> The ability of glycerol to trap metal catalysts most likely due to its supramolecular arrangement and the stability exhibited by both Pd<sup>[28]</sup> and Cu<sup>[29]</sup> based nanoparticles, encouraged us to study more challenging Ni(0) nanoparticles, with the aim of overcoming the surface oxidation and consequently obtaining suitable and reusable catalysts, leading to nickel-free products.

## Results and Discussion

**Synthesis and characterization of Ni(0) nanoparticles.** Zero-valent nickel nanoparticles (NiNPs) were synthesized by decomposition of the organometallic precursor [Ni(cod)<sub>2</sub>] in glycerol under hydrogen atmosphere (3 bar) at 100 °C, in the presence of different types of stabilizers (Ni/stabilizer = 1/1): quinidine (**A**), cinchonidine (**B**) and TPPTS (**C**), based on the methodology previously reported for palladium nano-systems (Scheme 1).<sup>[28]</sup> For the three NiNPs, black colloidal solutions were obtained. Lower pressure (1 bar) or lower temperature (80 °C) led to the formation of agglomerates (see Fig. S1 in the Supporting Information). Moreover, lower content on stabilizer (Ni/stabilizer = 1/0.5 and 1/0.3 for both TPPTS and quinidine) or in the absence of any stabilizer (it means, only in the presence of glycerol) did not led to stable colloidal solutions, observing the instantaneous precipitation of bulk metal under hydrogen pressure.

Ni(II) salts as metal precursors, such as Ni(OAc)<sub>2</sub> and Ni(NO<sub>3</sub>)<sub>2</sub>, led to green or yellow dissolutions depending on the stabilizer, suggesting the presence of Ni(II) species.



**Scheme 1.** Synthesis of Ni(0) nanoparticles **NiL** (**L** denotes the stabilizer) in glycerol from decomposition of [Ni(cod)<sub>2</sub>].

The as-prepared colloidal **NiA-NiC** solutions were analyzed by low resolution TEM. The obtained micrographs mainly showed the formation of small, spherical and quite well-dispersed NiNPs (1.1 - 1.3 ± 0.3 nm), together with few bigger particles (*ca.* 2 - 5 nm; Fig. 1).

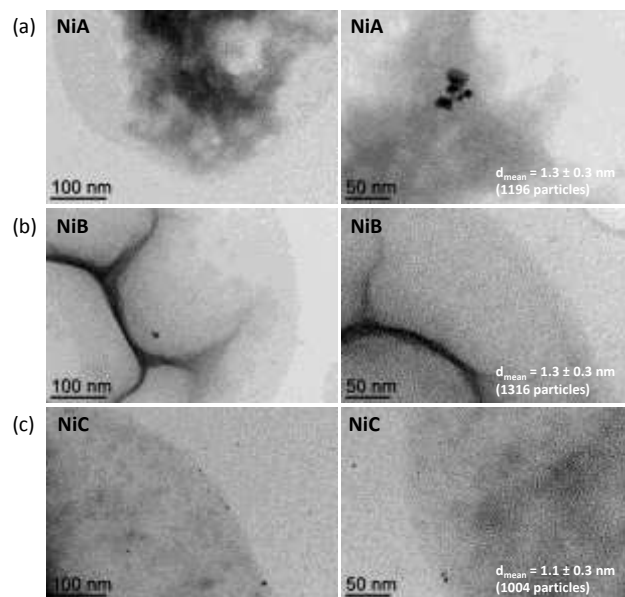


**Figure 1.** TEM images of **NiA** (a), **NiB** (b) and **NiC** (c) in glycerol. Mean diameters excluding the bigger particles.

With the aim of determining the structure of **NiA-NiC** in glycerol, HR-TEM analyses on those bigger nanoparticles only exhibited the presence of crystalline fcc Ni(0) particles, in contrast to hcp Ni(0) nanoparticles prepared in ionic liquids under thermal decomposition conditions (Fig. 2).<sup>[26]</sup> EDX analyses proved the presence of the corresponding stabilizers (Fig. 2). It is important to draw attention to the stability of Ni(0)NPs in glycerol. Therefore, the colloidal solution corresponding to **NiA** was exposed

to air and moisture for ten days; after this time, HR-TEM analysis revealed that NiNPs remained dispersed without any sign of agglomeration, showing the same crystalline structure (Fig. S2 in the Supporting Information); this test is coherent with the low solubility of molecular oxygen in glycerol.<sup>[30]</sup> Moreover, the synthesis of NiA was scaled-up ten times (50 mL of NiA colloidal solution), preserving size and morphology of nanoparticles (Fig. S3 in the Supporting Information), and catalytic reactivity (see below).

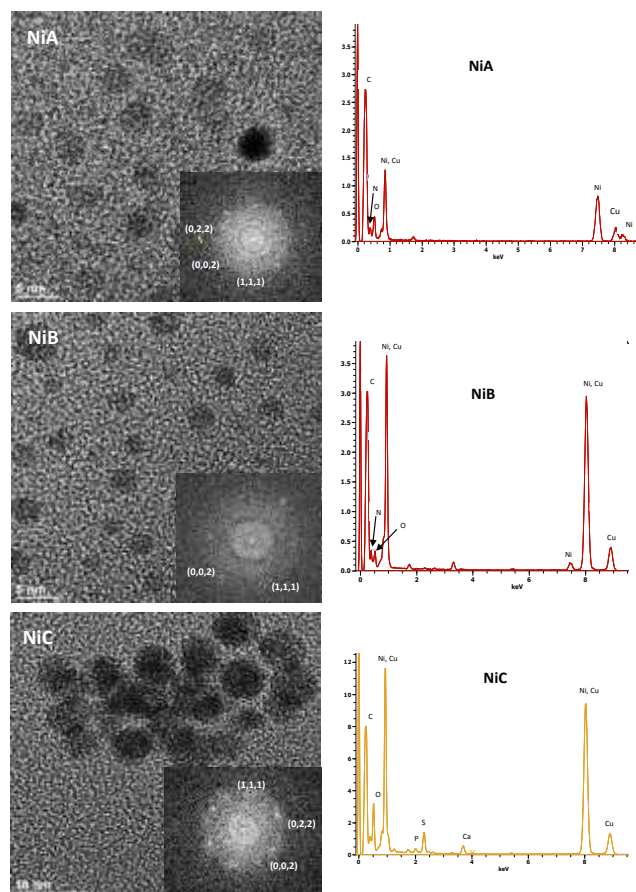


**Figure 2.** HR-TEM micrographs (left) and EDX analyses (right) of NiNPs in glycerol NiA, NiB and NiC in glycerol; inserts show the crystallographic planes (corresponding to fcc Ni(0) structure) observed by Fast Fourier Transform on selected nanoparticles.

NiNPs, NiA(s)-NiC(s), were isolated at solid state from the corresponding colloidal glycerol solutions by centrifugation. The obtained black powders were stocked in the glove-box to avoid their oxidation. Powder X-Ray Diffraction (PXRD) merely evidenced the fcc structure of nickel(0); small NiNPs (*ca.* 1 nm) could not be observed by PXRD and only large particles were detected (Fig. S4 in the Supporting Information). Their infrared spectra showed the presence of the corresponding ligand (Fig. S5 in the Supporting Information). In addition, the IR spectrum of NiC(s) excluded the presence of nickel oxide

(absence of any absorption band at 425-475  $\text{cm}^{-1}$  corresponding to Ni-O stretching<sup>[31]</sup>); however, NiNPs stabilized by cinchona-based alkaloids present absorption bands in the 550-400  $\text{cm}^{-1}$  range, hindering the observation of bands coming from nickel oxides (Fig. S5d in the Supporting Information). HR-TEM images of NiA(s)-NiC(s) at solid state did not exhibit any significant difference in relation to the analyses of NiA-NiC dispersed in glycerol, also showing Ni(0) crystalline phases (Fig. S6 in the Supporting Information).

Elemental and ICP-AES analyses gave similar metal/ligand ratio: Ni/stabilizer = 1/0.06 for both cinchona ligands (A and B) and 1/0.05 for the phosphine (C), which led to the idealized formula of Ni<sub>147</sub>A<sub>10</sub>, Ni<sub>147</sub>B<sub>15</sub> and Ni<sub>147</sub>C<sub>6</sub>, taking into account the compact fcc structure of these nanoparticles. With the aim of quantifying the content of hydrides present in the nanoparticles (molecular hydrogen was used as reducing agent in the synthesis of NiNPs), we carried out a hydrogen transfer reaction between the nanoparticles stabilized by quinidine, NiA(s), and phenylacetylene. The alkyne consumption to give styrene was monitored by <sup>1</sup>H NMR up to no further evolution was observed, resulting in a Ni/H ratio of 1/1.4 (Fig. S7 in the Supporting Information). This high hydride content can probably be due to the presence of interstitial hydrides in the nanocluster structure. Unfortunately, XPS analyses showed very low intense signals for the Ni 2p binding region, probably associated to a low electronic density on the surface related to the small size of particles together with the common surface defaults (Fig. S8 in the Supporting Information).

Magnetic measurements for Ni(0)NPs stabilized by quinidine were carried out, both in glycerol solution and solid state (Fig. 3). Actually, both materials exhibited narrow hysteresis at 2 K (coercive fields of 64 Oe and 89 Oe for NiA dispersed in glycerol and NiA(s), respectively), together with moderate remanence magnetizations (0.66 and 2.15 emu/g for NiA dispersed in glycerol and NiA(s), respectively), showing a weak ferromagnetic behavior. The saturation magnetization of NiA(s) (31 emu/g) is slightly lower than that reported for bulk nickel (54 emu/g)<sup>[32]</sup>. Data corresponding to NiA(s) is in agreement with that reported for cubic nickel nanocrystals.<sup>[33]</sup> The lower values of coercive fields and remanence magnetization of nickel nanoparticles in glycerol (NiA) than those observed for nanoparticles in solid state (NiA(s)) can be related to the higher amount of capping agents around the metal nanoparticles (*i.e.* both glycerol and quinidine), leading to a magnetic material constituted by a crystalline core surrounded by a “disordered” surface.<sup>[34]</sup>

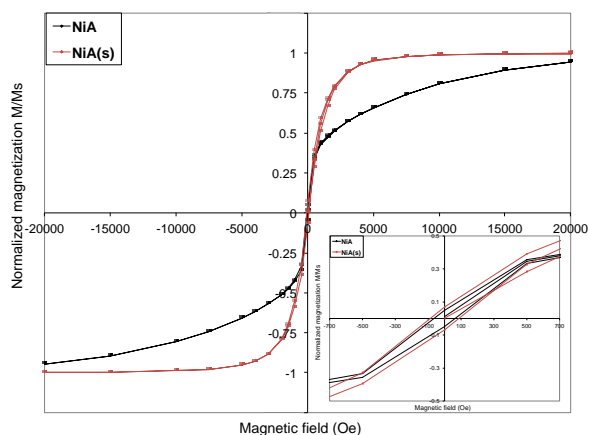


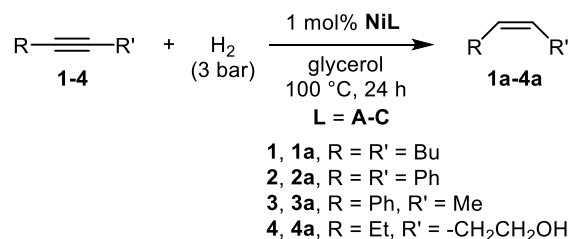
**Figure 3.** Magnetization curves of nickel nanoparticles stabilized by quinidine dispersed in glycerol (black line) and isolated NiNPs at solid state (red line) at 2 K.

**NiNPs catalyzed semihydrogenation reactions.** The work developed by Yus and co-workers using Ni(0) nanoparticles obtained *in situ* by reduction of nickel(II) salts in THF, led to a highly active catalytic system for the reduction of dienes and both internal and terminal alkynes, obtaining the corresponding alkenes in high yields under room conditions; however, this catalytic system could not be efficiently recycled.<sup>[7]</sup> Supported catalysts including Cu- and Ni-Al hydrotalcites,<sup>[9]</sup> nickel phosphide nanoparticles,<sup>[10]</sup> NiNPs decorated on polyaniline/graphite oxide composite<sup>[12]</sup> and Rh-Ni nanoflowers immobilized in a metal organic framework,<sup>[13]</sup> have been used for the selective hydrogenation of alkynes obtaining moderate to good yields, but generally under harsh conditions, showing unsuccessful catalyst recycling. Magnetic nano-Ni-Fe<sub>2</sub>O<sub>4</sub> catalyst<sup>[35]</sup> and magnetic amine-nickel complex coating Fe<sub>3</sub>O<sub>4</sub> nanoparticles allowed the recycling due to the easy separation of the catalyst.<sup>[8]</sup> NiGa bimetallic nanoparticles in imidazolium-based ionic liquid were active for the reduction of alkyl terminal alkynes and aryl internal alkynes, and the liquid support allows the recycling of the catalytic phase for at least 4 runs.<sup>[11]</sup>

With the aim of studying the selectivity on the hydrogenation of alkynes, we chose the hydrogenation of 5-decyne (**1**) to compare the reactivity of NiA-NiC (entry 1, Table 1). Under 3 bar of H<sub>2</sub> at 100 °C using 1 mol% of NiNPs in glycerol, full conversion was achieved after 2 h of reaction, exclusively obtaining 5-decene (**1a**). Using NiA prepared at large scale (50 mL scale; for all the other catalytic results, smaller synthesis scales were used, 5 or 10 mL scale), the same reactivity was observed than using smaller NiNPs synthesis scale (entry 1, Table 1). Other internal alkynes (**2-4**) led to the expected alkenes in high yields (**2a-4a**; entries 2-4, Table 1). The conversion for the hydrogenation of 3-phenylpropargyl alcohol was low (62%, using NiA as

catalyst), but highly chemo-selective towards the corresponding alkene (57% yield). Unfortunately, 1-(4-chlorophenyl)-2-phenylacetylene was nearly inactive at low hydrogen pressure (*ca.* 10% conversion using NiA as catalyst under 3 bar H<sub>2</sub>); under 20 bar H<sub>2</sub> pressure, a mixture of alkene/alkane of 75/25 was achieved (80% conversion).

**Table 1.** Semihydrogenation of internal alkynes catalyzed by NiNPs in glycerol.<sup>a)</sup>



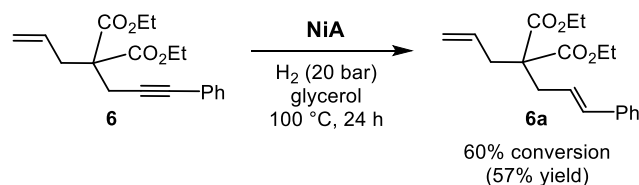
Entry	Substrate	NiA Conv. (yield) (%) <sup>b)</sup>	NiB Conv. (yield) (%) <sup>b)</sup>	NiC Conv. (yield) (%) <sup>b)</sup>
1 <sup>c)</sup>	<b>1</b>	>99 (98) <sup>d)</sup>	>99 (97)	98 (94)
2	<b>2</b>	>99 (90)	>99 (98)	93 (90)
3	<b>3</b>	88 (84)	85 (80)	78 (74)
4	<b>4</b>	98 (96)	94 (91)	89 (87)
5 <sup>e),f)</sup>	<b>5</b>	92 (89)	93 (89)	89 (84)

<sup>a)</sup> Results from duplicated experiments. No reactivity in the absence of metal and/or stabilizer. Reaction conditions: 1 mmol of substrate (**1-4**) and 1 mL of the catalytic glycerol solution of NiA-NiC (10<sup>-2</sup> mol L<sup>-1</sup>, 0.01 mmol of total Ni; determined by ICP). <sup>b)</sup> Determined by GC and GC-MS using decane as internal standard. <sup>c)</sup> Cyclooctane used as internal standard. <sup>d)</sup> Using large scale synthesis of NiA (50 mL scale), 97% conversion and 94% yield of **1a** was obtained. <sup>e)</sup> Substrate **5** corresponds to phenylacetylene (see Table 2). <sup>f)</sup> Under 1 bar of H<sub>2</sub>.

The stereochemistry of the unsymmetrically substituted alkene **3a** was established by a NOESY-NMR experiment, evidencing the exclusive formation of the (*Z*)-stereoisomer (Fig. S9 in the Supporting Information); this fact points to a *syn* hydrogen addition, following a Horiuti-Polanyi mechanism.<sup>[36]</sup> No important differences were observed among the three catalysts employed, showing a slightly better performance for those containing a cinchona stabilizer (NiA, NiB) in relation to that stabilized by the phosphine TPPTS (NiC); this trend was also noticed for the phenylacetylene hydrogenation to give styrene (entry 5, Table 1). The over-reduction to afford the corresponding saturated product was only observed under harsher conditions; actually, full conversion of diphenylacetylene took place under 20 bar H<sub>2</sub> at 100 °C using 5 mol% NiA, leading to a

mixture of stilbene/1,2-diphenylethane (90/10 ratio respectively) after 24 h of reaction. When these catalysts (**NiA-NiC**, see Scheme S1 in the Supporting Information) were applied in the hydrogenation of 4-phenyl-3-buten-2-one, no reaction was observed, in contrast to the recent published NiNPs stabilized by carboxylic acids and supported on silica, where the corresponding butanone was obtained under smooth conditions.<sup>[24]</sup> The high selectivity observed by **NiA-NiC** towards the semihydrogenation process, evidences the effect of the capping agents (**A-C**), hindering the coordination of alkenes to the surface, in agreement with the higher adsorption enthalpies for internal alkynes than for internal alkenes.<sup>[37]</sup>

Hydrogenation of the 1,6-enyne **6a** gave exclusively the corresponding diene under high pressure (20 bar H<sub>2</sub>), without observing the reduction of either of the two alkene groups (Scheme 2).



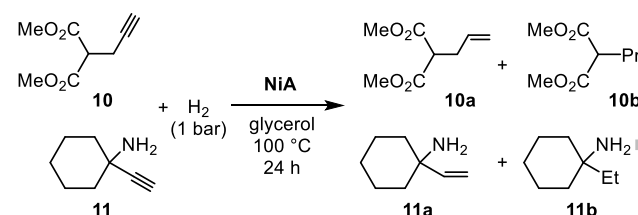
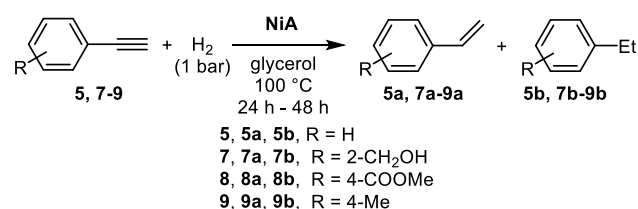
**Scheme 2.** Hydrogenation of the 1,6-enyne **6** catalyzed by **NiA**.

Terminal alkynes (**5**, **7-9**) selectively gave the corresponding styrene derivative under low hydrogen pressure (1 bar H<sub>2</sub>, 1 mol% **NiA**, 24 h; entries 1-3, Table 2), except for **9** where a mixture of styrene and ethylbenzene derivatives were formed (**9a/9b** = 85/15, entry 4, Table 2). However, working at higher catalyst load (5 mol%) and longer times (up to 48 h), full hydrogenation was favored towards the corresponding alkyl-benzene derivative (entries 5-8, Table 2), in contrast to that observed for internal alkynes **1-4**. The preferred over-reduction for terminal alkynes can be presumed by the faster hydrogenation of both terminal alkynes and alkenes on the metal surfaces than that observed for internal ones, mainly due to coordination constraints at the nanoparticle surface.<sup>[37]</sup> For non-aromatic substrates, such as alkynes **10** and **11**, the full reduction of the C-C triple bond was favored even using low catalyst load (entries 9 and 10, Table 2).

It is noteworthy that even in the presence of a hydroxyl or amino group (alkynes **7**, **10** and **11**), the full hydrogenation of the C-C triple bond was favored (entries 6, 9 and 10, Table 2), in contrast to the behavior observed using iron nanoparticles, where the formation of alkenes was preferred, due to the coordination of the OH group at the surface.<sup>[38]</sup> In our case, glycerol probably prevents the coordination of OH and NH<sub>2</sub> groups to the metal surface by hydrogen

bond interaction, favoring the over-reduction of the alkyne.

**Table 2.** Hydrogenation of terminal alkynes catalyzed by **NiA** in glycerol.<sup>a)</sup>



Entry	Substrate	<b>NiA</b> (mol%)	Conv. (%) <sup>b)</sup>	Selectivity ( <b>a/b</b> ) <sup>b),c)</sup>
1 <sup>d)</sup>	<b>5</b>	1	92	100/0 (89)
2 <sup>d)</sup>	<b>7</b>	1	69	100/0 (66)
3 <sup>d)</sup>	<b>8</b>	1	71	100/0 (68)
4 <sup>d)</sup>	<b>9</b>	1	98	85/15
5 <sup>d)</sup>	<b>5</b>	5	95	15/85
6 <sup>e)</sup>	<b>7</b>	5	94	0/100 (90)
7 <sup>e)</sup>	<b>8</b>	5	97	0/100 (95)
8 <sup>d)</sup>	<b>9</b>	5	94	0/100 (91)
9 <sup>d)</sup>	<b>10</b>	1	100	40/60
10 <sup>d)</sup>	<b>11</b>	1	90	25/75

<sup>a)</sup> Results from duplicated experiments. No reactivity in the absence of metal and/or stabilizer. Reaction conditions: 1 mmol (for 1 mol%) or 0.2 mmol (for 5 mol%) of substrate (**5-7**) and 1 mL of the catalytic glycerol solution of **NiA** (10<sup>-2</sup> molL<sup>-1</sup>, 0.01 mmol of total Ni; determined by ICP). <sup>b)</sup> Determined by GC and GC-MS using decane as internal standard. <sup>c)</sup> Yields given in brackets. <sup>d)</sup> For 24 h. <sup>e)</sup> For 48 h.

The catalytic glycerol phase was recycled at least ten times, preserving its catalytic behavior, as shown for the semihydrogenation of 5-decyne (Fig. 4). No presence of nickel in the extracted organic product was evidenced by ICP-AES analyses after the 1<sup>st</sup>, 4<sup>th</sup> and 10<sup>th</sup> runs; neither significant differences by TEM were observed for the catalytic phase after the 1<sup>st</sup> and 8<sup>th</sup> runs (Fig. S10 in the Supporting Information). Therefore, the metal trapping effect of glycerol avoids the leaching of nickel from the catalytic solution and hence metal-free compounds can be obtained, valuable aspect taking into account the nickel toxicity.<sup>[39]</sup>

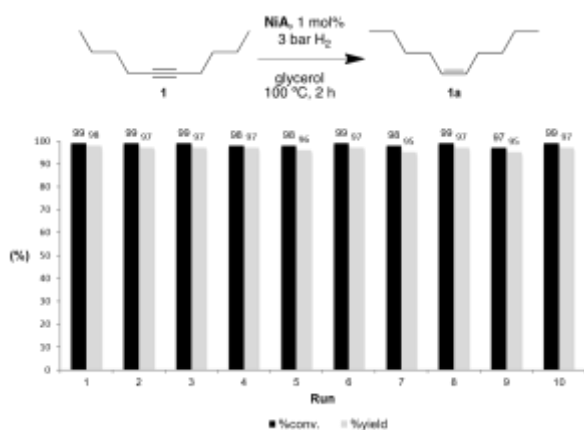


**Figure 4.** NiA-catalyzed semihydrogenation of 5-decyne (**1**), showing the recycling of the catalytic phase up to ten runs. For catalytic conditions, see entry 1 of Table 1.

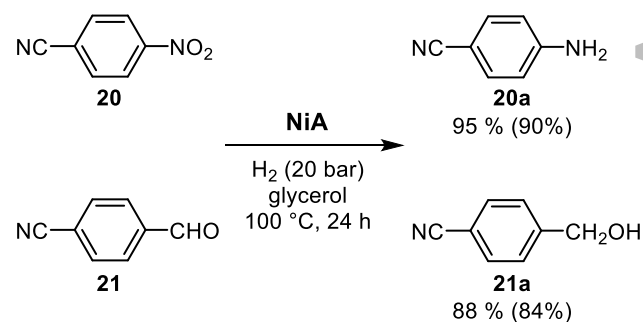
We were also interested in the reduction of other types of functions, such as nitro-, nitrile- and formyl-substituted aromatics. In the literature, NiNPs have been applied in the reduction of nitro-substituted aromatic compounds, including NiPd bimetallic nanoparticles.<sup>[40]</sup> Monometallic Ni(0)-based nanoparticles supported on different types of supports led to the formation of anilines under harsh conditions,<sup>[41-43]</sup> giving over-reduction of the aromatic rings<sup>[42]</sup> and by-products coming from the reaction of the formed anilines and stabilizers of the nanocatalysts.<sup>[43]</sup> However, few NiNPs colloidal systems have been used,<sup>[18,44]</sup> probably due to the easy oxidation of the catalyst, losing its catalytic activity.

With the aim of evaluating our NiNPs dispersed in glycerol, we first studied their catalytic behaviour in the hydrogenation of nitro-derivatives. In comparison with the hydrogenation of alkynes (see above), higher catalyst load was required (5 mol% Ni) for the reduction of these functional groups. Analogously to the trend observed for alkyne hydrogenations, NiNPs stabilized by TPPTS were much less efficient than those containing cinchona ligands as stabilizers, NiA and NiB (see Table 3), probably due to the stronger interaction of the phosphine to the Ni surface, hampering the coordination of the substrate to the metal. Nitrobenzene (**12**) and 4-nitrophenol (**13**) were efficiently hydrogenated by NiNPs stabilized by cinchona ligands (NiA and NiB), giving high yield of the corresponding aniline derivative, **12a** and **13a**, under low H<sub>2</sub> pressure (3 bar; entries 1-2, Table 3). Curiously, 1,3-dinitrobenzene (**14**) was hydrogenated by NiA obtaining 1,3-diaminobenzene (**14a**) in 77% yield (entry 3, Table 3), however, NiB was substantially less active (only 30% yield under the same conditions). This behavior can be attributed to two related effects: stabilizer A is probably more labile than B due to the presence of the methoxide group on the quinoline ring, hence favoring the coordination of substrate to be hydrogenated, effect

that may have a greater impact on sterically hindered substrates, such as 1,3-dinitrobenzene (**14**).

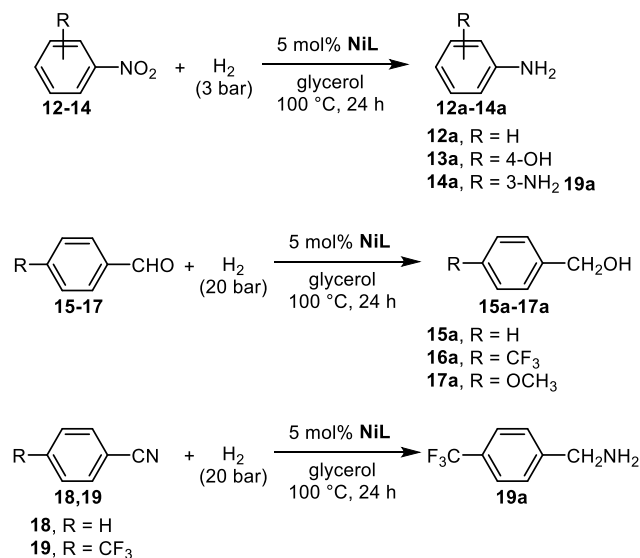
For benzaldehyde derivatives (**15-17**), higher hydrogen pressure (20 bar) was required to achieve good yields in benzyl alcohols (up to 92%, entries 4-6, Table 3) with both catalysts NiA and NiB. No formation of acetal coming from the reaction between aldehyde and glycerol was detected, in contrast to that observed using NiC (entries 4 and 6, Table 3). For this latter catalyst, only when the hydrogenation is faster, such as for 4-trifluoromethylbenzaldehyde (**16**; entry 5, Table 3), the formation of the corresponding acetal was precluded. NiA also hydrogenated hexanal, giving 1-hexanol in moderate yield (35%). Unfortunately, NiA catalyst was not active in the hydrogenation of acetophenone. The synthesis of benzylamines by hydrogenation of nitriles was possible when 4-trifluoromethylbenzonitrile (**19**) was used as substrate (entry 8, Table 3). In the case of 4-methylbenzonitrile, no reaction was observed using any of the three catalysts; for benzonitrile (**18**; entry 7, Table 3), only a mixture of dibenzylamine and *N*-benzylidenebenzylamine was obtained (see Fig. S11 in the Supporting Information), common by-products in the hydrogenation of nitriles.<sup>[45]</sup>

Benzonitriles containing formyl or nitro groups, such as 4-nitrobenzonitrile (**20**) and 4-formylbenzonitrile (**21**) were selectively hydrogenated towards the corresponding aniline (**20a**) and benzyl alcohol (**21a**), using NiA as catalyst, preserving the nitrile moiety (Scheme 3). Nitro (**20**) and formyl (**21**) groups are faster reduced than nitrile function. The resulting aniline **20a** and benzyl alcohol **21a** disfavors the reduction of CN group because of the electron-donor character of NH<sub>2</sub> and CH<sub>2</sub>OH groups, in agreement with the lack of reactivity observed for 4-methylbenzonitrile (see Scheme S2 in the Supporting Information), and in agreement with the behavior observed using bimetallic CuNi nanoparticles in the hydrogenation of nitriles containing nitro groups, as recently reported by Sun and co-workers.<sup>[46]</sup>



**Scheme 3.** NiA catalyzed hydrogenation of benzonitriles **20** and **21** (figures indicate conversions (yields) determined by GC using decane as internal standard)

**Table 3.** NiNPs in glycerol catalyzed hydrogenation of aromatic substrates containing nitro, formyl and nitrile functional groups.<sup>a)</sup>



Entry	Substrate (R)	NiA Conv. (yield) (%) <sup>b)</sup>	NiB Conv. (yield) (%) <sup>b)</sup>	NiC Conv. (yield) (%) <sup>b)</sup>
1	<b>12</b> (H)	90 (89)	96 (91)	31 (27)
2	<b>13</b> (4-OH)	98 (95)	91 (88)	30 (26)
3	<b>14</b> (3-NO <sub>2</sub> )	80 (77)	35 (30)	<5
4	<b>15</b> (H)	95 (92)	93 (89)	77 (30) <sup>c)</sup>
5	<b>16</b> (4-CF <sub>3</sub> )	95 (90)	94 (90)	75 (70)
6	<b>17</b> (4-OMe)	90 (87)	83 (78)	71 (25) <sup>d)</sup>
7	<b>18</b> (H)	95 (70/30) <sup>e)</sup>	95 (20/80) <sup>f)</sup>	<5
8	<b>19</b> (4-CF <sub>3</sub> )	95 (92)	89 (82)	<5

<sup>a)</sup> Results from duplicated experiments. No reactivity in the absence of metal and/or stabilizer. Reaction conditions: 0.2 mmol of substrate (**9-16**) and 1 mL of the catalytic glycerol solution of NiA-NiC (10<sup>-2</sup> molL<sup>-1</sup>, 0.01 mmol of total Ni; determined by ICP). <sup>b)</sup> Determined by GC and GC-MS using decane as internal standard. <sup>c)</sup> 40% formation of the five-membered acetal coming from the reaction of aldehyde **12** and glycerol. <sup>d)</sup> 40% formation of the five-membered acetal coming from the reaction of aldehyde **14** and glycerol. <sup>e)</sup> *N*-benzylidenebenzylamine/dibenzylamine ratio = 70/30. <sup>f)</sup> *N*-benzylidenebenzylamine/dibenzylamine ratio = 20/80.

## Conclusions

For the first time, highly stable zero-valent NiNPs were efficiently synthesized and trapped in neat glycerol. The nanomaterials were obtained under

smooth conditions by a single step methodology, using three different stabilizers (TPPTS and two cinchona-based alkaloids, quinidine and cinchonidine), and fully characterized both in glycerol solution and solid state. The as-prepared nanocatalysts were highly selective for the hydrogenation of alkyl and aryl alkynes without reducing neither conjugated C=C bonds nor aromatic rings. In addition, nitro aromatic compounds, benzonitrile derivatives and formyl containing compounds were reduced under relatively mild conditions. Studies concerning the synthesis of bimetallic nanocatalysts in glycerol are currently under investigation, with the aim of being applied in the synthesis of fine chemicals.

## Experimental Section

**Synthesis of NiNPs in glycerol, NiA-NiC.** 0.05 mmol (13.6 mg) of [Ni(cod)<sub>2</sub>] and 0.05 mmol of ligand (14.7 mg for quinidine (**A**); 16 mg for cinchonidine (**B**); 28.4 mg for TPPTS (**C**)) were dissolved in 5 mL of glycerol and stirred under argon in a Fisher-Porter bottle at room temperature until complete dissolution. The system was then pressurized under 3 bar of dihydrogen and stirred at 100 °C for 18 h. A black colloidal solution was then obtained.

**Isolation of NiNPs from the glycerol solution.** The as-prepared NiNPs in glycerol were transferred to a centrifugation tube under argon. Centrifugation was carried out at 5,000 rpm for 15 min and the solution was then separated by decantation. This process was repeated 3 times until complete removal of glycerol. The remaining black powder was then dried under vacuum at 80 °C overnight. Elementary analysis (nickel load determined by ICP-AES): **NiA**: Ni 73.1%, C 22.5%, H 1.7%, N 2.7%; **NiB**: Ni 67.1%, C 27.2%, H 2.3%, N 3.4%; **NiC**: Ni 74.9%, C 16.9%, H 0.8%, S 7.4%. Expected data for proposed nanoclusters: **Ni<sub>147</sub>A<sub>10</sub>**: Ni 72.7%, C 20.2%, H 2.0%; N 2.4%; **Ni<sub>147</sub>B<sub>15</sub>**: Ni 66.15%, C 26.2%, H 2.55%; N 3.2%; **Ni<sub>147</sub>C<sub>6</sub>**: Ni 71.7%, C 10.8%, H 0.6%; S 4.8%;

**Hydride titration of NiA.** Isolated NiA nanoparticles (0.1 mmol, 6 mg) were dispersed in 0.6 mL of THF-*d*<sub>8</sub> in a Young NMR tube and then phenylacetylene (0.1 mmol, 10 mg) was added, in the presence of an external standard (0.1 mmol, 12 mg of cyclooctane). The formation of styrene was monitored by <sup>1</sup>H NMR.

**General procedure for NiNPs-catalyzed hydrogenation in glycerol.** In a Fisher-Porter bottle (from 1 to 3 bar) or an autoclave (from 4 to 20 bar), the appropriate substrate (1 mmol for 1 mol% of catalyst or 0.2 mmol for 5 mol%) was added to 1 mL of preformed nickel nanoparticles in glycerol under argon (total amount of nickel: 0.01 mmol). The reaction mixture was treated under vacuum and then pressurized with H<sub>2</sub> at the appropriate pressure, heated up to the desired temperature, stirred for the established time,

and then cooled down to room temperature. Organic products were extracted from glycerol with dichloromethane (5 x 3 mL) and the solvent was evaporated under vacuum. All the products were identified by GC-MS analysis, <sup>1</sup>H and <sup>13</sup>C NMR spectroscopy, comparing with the reported data.

### General procedure for recycling of the catalytic phase.

After extraction of the organic products, the catalytic phase was treated under vacuum at 50 °C for 2 h and the appropriated reagents were then added under argon to the catalytic phase. The reaction mixture was pressurized with H<sub>2</sub> at the appropriated pressure, heated up to the desired temperature, stirred for the established time, and then cooled down to room temperature. Organic products were extracted from glycerol with dichloromethane (5 x 3 mL) and dried under reduced pressure. This process was repeated for each of the different runs.

## Acknowledgements

The Centre National de la Recherche Scientifique (CNRS) and Université de Toulouse 3 - Paul Sabatier are gratefully acknowledged for financial support. A. R. thanks the CONACYT Mexican agency for the PhD scholarship.

## References

- [1] For selected reviews, see: a) J. A. Delgado, O. Benkirane, C. Claver, D. Curulla-Ferré, C. Godard, *Dalton Trans.* **2017**, 46, 12381-12403; b) A. Molnár, A. Sárkány, M. Varga, *J. Mol. Catal. A: Chem.* **2001**, 173, 185-221.
- [2] For selected contributions, see: a) A. Borodzinski, G. C. Bond, *Catal. Rev. Sci. Eng.* **2006**, 48, 91-144; b) J. A. Garduño, A. Arévalo, J. J. García, *Dalton Trans.* **2015**, 44, 13419-13438.
- [3] a) H. Lindlar, *Helv. Chim. Acta* **1952**, 35, 446-450; b) H. Lindlar, R. Dubuis, *Org. Synth.* **1966**, 46, 89-91.
- [4] a) P. T. Witte, P. H. Berben, S. Boland, E. H. Boymans, D. Vogt, J. W. Geus, J. G. Donkervoort, *Top. Catal.* **2012**, 55, 505-511; b) B. S. Takale; X. Feng; Y. Lu; M. Bao; T. Jin; T. Minato; Y. Yamamoto, *J. Am. Chem. Soc.* **2016**, 32, 10356-10364; c) F. Chen, C. Kreyenschulte, J. Radnik, H. Lund, A.-E. Surkus, K. Junge, M. Beller, *ACS Catal.* **2017**, 7, 1526-1532; d) Y. Lu, X. Feng, B. S. Takale, Y. Yamamoto, W. Zhang, M. Bao, *ACS Catal.* **2017**, 7, 8296-8303.
- [5] P. Gallois, J.-J. Brunet, P. Caubere, *J. Org. Chem.* **1980**, 45, 1946-1950.
- [6] D. Savoia, E. Tagliavini, C. Trombini, A. Umami-Ronchi, *J. Org. Chem.* **1981**, 46, 5340-5343.
- [7] a) F. Alonso, I. Osante, M. Yus, *Adv. Synth. Catal.* **2006**, 348, 305-308; b) F. Alonso, I. Osante, M. Yus, *Tetrahedron* **2007**, 63, 93-102; c) F. Alonso, J. J. Calvino, I. Osante, M. Yus, *Chem. Lett.* **2005**, 34, 1262-1263.
- [8] V. Polshettiwar, B. Baruwati, R. S. Varma, *Green Chem.* **2009**, 11, 127-131.
- [9] B. Bridier, N. López, J. Pérez-Ramírez, *J. Catal.* **2010**, 269, 80-92.
- [10] S. Carencó, A. Leyva-Pérez, P. Concepción, C. Boissière, N. Mézailles, C. Sánchez, A. Corma, *Nano Today* **2012**, 7, 21-28.
- [11] K. Schütte, A. Doddi, C. Kroll, H. Meyer, C. Wiktor, C. Gemel, G. van Tendeloo, R. A. Fischer, C. Janiak, *Nanoscale* **2014**, 6, 5532-5544.
- [12] V. Panwar, A. Kumar, R. Singh, P. Gupta, S. S. Ray, S. L. Jain, *Ind. Eng. Chem. Res.* **2015**, 54, 11493-11499.
- [13] L. Chen, H. Li, W. Zhan, Z. Cao, J. Chen, Q. Jiang, Y. Jiang, Z. Xie, Q. Kuang, L. Zheng, *ACS Appl. Mater. Interfaces* **2016**, 8, 31059-31066.
- [14] G. Marzun, A. Levish, V. Mackert, T. Kallio, S. Barcikowski, P. Wagener, *J. Coll. Inter. Sci.* **2017**, 489, 57-67.
- [15] J. Aguilhon, C. Thomazeau, C. Boissière, O. Durupthy, C. Sanchez, *Part. Part. Syst. Charact.* **2013**, 30, 532-541.
- [16] K. Anic, A. Wolfbeisser, H. Li, C. Rameshan, K. Föttinger, J. Bernardi, G. Rupprechter, *Top. Catal.* **2016**, 59, 1614-1627.
- [17] Ö. Metin, V. Mazumder, S. Özkar, S. Sun, *J. Am. Chem. Soc.* **2010**, 132, 1468-1469.
- [18] D. Baudoin, K. Chung Szeto, P. Laurent, A. De Mallmann, B. Fenet, L. Veyre, U. Rodemerck, C. Copéret, C. Thieuleux, *J. Am. Chem. Soc.* **2012**, 134, 20624-20627.
- [19] E. J. Roberts, S. E. Habas, L. Wang, D. A. Ruddy, E. A. White, F. G. Baddour, M. B. Griffin, J. A. Schaidle, N. Malmstadt, R. L. Brutchey, *ACS Sustainable Chem. Eng.* **2017**, 5, 632-639.
- [20] A. P. LaGrow, B. Ingham, S. Cheong, G. V. M. Williams, C. Dotzler, M. F. Toney, D. A. Jefferson, E. C. Corbos, P. T. Bishop, J. Cookson, R. D. Tilley, *J. Am. Chem. Soc.* **2012**, 134, 855-858.
- [21] J. Park, E. Kang, S. U. Son, H. M. Park, M. K. Lee, J. Kim, K. W. Kim, H.-J. Noh, J.-H. Park, C. J. Bae, J.-G. Park, T. Hyeon, *Adv. Mater.* **2005**, 17, 429-434.
- [22] E. G. C. Neiva, M. F. Bergamini, M. M. Oliveira, L. H. Marcolino Jr., A. J. G. Zarbin, *Sens. Actuators, B* **2014**, 196, 574-581.
- [23] a) T. O. Ely, C. Amiens, B. Chaudret, *Chem. Mater.* **1999**, 11, 526-529; b) N. Cordente, M. Respaud, F. Senocq, M.-J. Casanove, C. Amiens, B. Chaudret, *Nano Lett.* **2001**, 1, 565-568.
- [24] L. Zaramello, B. L. Albuquerque, J. B. Domingos, K. Philippot, *Dalton Trans.* **2017**, 46, 5082-5090.
- [25] P. Migowski, G. Machado, S. R. Texeira, M. C. M. Alves, J. Morais, A. Traverse, J. Dupont, *Phys. Chem. Chem. Phys.* **2007**, 9, 4814-4821.

- [26] S. Wegner, C. Rutz, K. Schütte, J. Barthel, A. Bushmelev, A. Schmidt, K. Dilchert, R. A. Fischer, C. Janiak, *Chem. Eur. J.* **2017**, *23*, 6330-6340.
- [27] Y. Li, M. Cai, J. Rogers, Y. Xu, W. Shen, *Mater. Lett.* **2006**, *60*, 750-753.
- [28] For Pd-based systems, see: a) F. Chadoura, C. Pradel, M. Gómez, *Adv. Synth. Catal.* **2013**, *355*, 3648-3660; b) F. Chadoura, S. Mallet-Ladeira, M. Gómez, *Org. Chem. Front.* **2015**, *2*, 312-318; c) A. Reina, C. Pradel, E. Martin, E. Teuma, M. Gómez, *RSC Adv.* **2016**, *6*, 93205-93216.
- [29] For Cu-based systems, see: a) F. Chadoura, C. Pradel, M. Gómez, *ChemCatChem* **2014**, *6*, 2929-2936; b) T. Dang-Bao, C. Pradel, I. Favier, M. Gómez, *Adv. Synth. Catal.* **2017**, *359*, 2832-2846.
- [30] I. Kutsche, G. Gildehaus, D. Schuller, A. Schumpe, *J. Chem. Eng. Data.* **1984**, *29*, 286-287.
- [31] M. A. Vidales-Hurtado, A. Mendoza-Galván, *Mater. Chem. Phys.* **2008**, *107*, 33-38.
- [32] a) T. Ishizaki, K. Yatsugi, K. Akedo, *Nanomaterials* **2016**, *6*, 172-184; b) I. M. L. Billas, A. Châtelain, W. A. de Heer, *Science* **1994**, *265*, 1682-1684.
- [33] M. Han, Q. Liu, J. He, Y. Song, Z. Xu, J. Zhu, *Adv. Mater.* **2007**, *19*, 1096-1100.
- [34] G. C. Papaefthymiou, *Nano Today*, **2009**, *4*, 438-447.
- [35] S. Payra, A. Saha, S. Banerjee, *RSC Adv.* **2016**, *6*, 52495-52499.
- [36] a) I. Horiuti, M. Polyani, *Trans. Faraday Soc.* **1934**, *30*, 1164-1172; b) G. C. Bond, *Metal-catalyzed reactions of hydrocarbons*, Springer, New York, **2005**.
- [37] *Supported Metals in Catalysis*, 2<sup>nd</sup> Edition, Eds. J. A. Anderson, M. Fernández García, Imperial College Press, London, **2012**.
- [38] V. Kelsen, B. Wendt, S. Werkmeister, K. Junge, M. Beller, B. Chaudret, *Chem. Commun.* **2013**, *49*, 3416-3418.
- [39] For the toxicity of nickel, see the following website of the European Chemicals Agency (ECHA): <https://echa.europa.eu/substances-restricted-under-reach/-/dislist/details/0b0236e1807e266a>
- [40] R. Raja, V. B. Golovko, J. M. Thomas, A. Berenguer-Murcia, W. Zhou, S. Xie, B. F. G. Johnson, *Chem. Commun.* **2005**, 2026-2028.
- [41] M. A. Harrad, B. Boualy, L. E. Firdoussi, A. Mehdi, C. Santi, S. Giovagnoli, M. Nocchetti, M. A. Ali, *Catal. Commun.* **2013**, *32*, 92-100.
- [42] X.-H. Lu, X.-L. Wei, D. Zhou, H.-Z. Jiang, Y.-W. Sun, Q.-H. Xia, *J. Mol. Catal. A* **2015**, *396*, 196-206.
- [43] L. Tarpani, E. Mencarelli, M. Nocchetti, L. Fanò, L. Taglieri, L. Latterini, *Catal. Commun.* **2016**, *74*, 28-32.
- [44] R. Xu, T. Xie, Y. Zhao, Y. Li, *Nanotechnology* **2007**, *18*, 055602-055606.
- [45] A. Galán, J. de Mendoza, P. Prados, J. Rojo, A. M. Echavarren, *J. Org. Chem.* **1991**, *56*, 452-454.
- [46] C. Yu, J. Fu, M. Muzzio, T. Shen, D. Su, J. Zhu, S. Sun, *Chem. Mater.* **2017**, *29*, 1413-1418.

## FULL PAPER

## Highly Stable Zero-Valent Nickel Nanoparticles in Glycerol: Synthesis and Applications in Selective Hydrogenations

*Adv. Synth. Catal.* **Year**, *Volume*, Page – PageAntonio Reina,<sup>a</sup> Christian Pradel,<sup>a</sup> and Montserrat Gómez<sup>a\*</sup>